Supporting information for

Unprecedented induced axial chirality in a molecular BODIPY dye: strongly bisignated electronic circular dichroism in the visible region

Esther M. Sánchez-Carnerero,[a] Florencio Moreno, [a] Beatriz L. Maroto, [a] Antonia R. Agarrabeitia, [a] Jorge Bañuelos, [b] Teresa Arbeloa, [b] Iñigo López-Arbeloa,[b] María J. Ortiz*[a] and Santiago de la Moya*[a]

[a] *Departamento de Química Orgánica I, Facultad de Ciencias Químicas, Universidad Complutense de Madrid, Ciudad Universitaria s/n, 28040, Madrid, Spain. Fax:+34 91 394 4103; Tel: +34 91 394 5090; E-mail: santmoya@ucm.es*

[b] *Departamento de Química Física, Universidad del Pais Vasco-EHU, Apartado 644, 48080, Bilbao, Spain.*

Table of contents

1. Experimental Section

1.1. Materials, instrumentation and techniques

Common solvents were dried and distilled by standard procedures. All starting materials and reagents were obtained commercially and used without further purifications. Flash chromatography purifications were performed on silica gel (230-400 mesh ASTM). Melting points are uncorrected. Thin-layer chromatography was performed on silica gel plates (silica gel 60, F254, supported on aluminium). NMR spectra were recorded at 20 ºC and the residual solvent peaks were used as internal standards. FTIR spectra were obtained from neat samples using the ATR technique. Mass spectra (MS) and high resolution mass spectrometry (HRMS) were performed using the EI technique. Optical rotations were recorded in a Perkin-Elmer (model 241) polarimeter (*c* are expressed in g / 100 mL, unless other units were indicated). UV-Vis absorption and fluorescence spectra were recorded in a Varian (model CARY 4E) spectrophotometer and a Spex FluoroLog 3-22 spectrofluorimeter, respectively. CD spectra were recorded in a Jasco (model J-715) spectropolarimeter using standard quartz cells of 1 cm optical path length. Fluorescence quantum yields (ϕ) were obtained using PM567 in ethanol as reference (ϕ^f = 0.84). Radiative decay curves were registered with the time correlated single-photon counting technique (Edinburgh Instruments, model FL920, with picosecond time-resolution) after excitation at 470 nm by means of a diode laser (PicoQuant, model LDH470). Fluorescence lifetimes (τ) were obtained after the deconvolution of the instrumental response signal from the recorded decay curves, by means of an iterative method.

1.2. Computational methods

Ground state geometries were optimized at the B3LYP theory level using the double valence basis set (6-31g), as implemented in popular Gaussian 09. The geometries were considered as energy minimum when the corresponding frequency analysis did not afford any negative value. The solvent effect was also simulated during the calculations by the Self Consistent Reaction Field (SCRF) using the Polarizable

Continuum Model (PCM). Chloroform was chosen as the solvent for the simulations, for a better comparison with the experimental measurements. For the conformational study of **1a**, **1b** and **1c**, a starting geometry with the BODIPY chromophores disposed in a coaxial arrangement (similar to that drawn in Fig. S1 for **1a**) was used for the optimization. The found fully-optimized helical geometries (only for **1a** and **1b**), with a preferred axial configuration (see Fig. S7), were submitted to plane reflection, and the chiral centres of the obtained mirror images inverted, to obtain the corresponding axially-complementary (diastereomeric) helices, which were used as starting geometries to be fully optimized. All the optimizations were conducted without any geometrical restriction, and carried out in a computational cluster provided by the SGIker resources of the UPV/EHU.

1.3. Synthetic procedure and characterization data

A mixture of 3,5-dichloro-8-(4-methylphenyl)-*F*-BODIPY (70.2 mg, 0.20 mmol), the corresponding 1,2-diphenyl-1,2-ethanodiamine stereoisomer (23.3 mg, 0.11 mmol) and triethylamine (22.2 mg, 0.22 mmol) in dry acetonitrile was stirred under argon for 24 h (see Fig. S1). The solvent was removed under reduced pressure and the residue purified by flash chromatography (hexane/CH_2Cl_2 1:1 to elute **1**, followed by pure CH_2Cl_2 to elute **2a** and **2b**, or CH_2Cl_2/AcOEt 9:1 to elute **2c**).

1a:

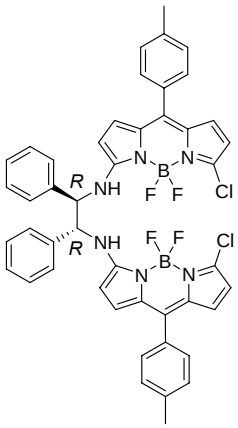

Yield: 41 mg, 49%. R_f = 0.22 (hexane/Et_2O 6:4). $[\alpha]_D^{20}$ –5696.4 (*c* 6.8 x 10^{-2}, $CHCl_3$). ^{1}H NMR ($CDCl_3$, 300 MHz) δ 7.39-7.32 (m, 6H); 7.28 and 7.22 (AB system, *J* = 7.8 Hz, 8H), 7.09-7.02 (m, 4H), 6.95 (br s, 2H), 6.82 (d, *J* = 4.9 Hz, 2H), 6.41 (d, *J* = 3.9 Hz, 2H), 6.21 (d, *J* = 3.9 Hz, 2H), 6.05 (d, *J* = 4.9 Hz, 2H), 5.04 (m, 2H), 2.42 (s, 6H) ppm. ^{13}C NMR ($CDCl_3$, 75 MHz) δ 160.3, 139.6, 135.8, 135.1, 134.0, 132.8, 132.0, 131.1, 130.6, 130.2, 129.2, 129.0, 128.9, 127.5, 121.7, 113.2, 110.5, 62.5, 21.3 ppm. FTIR ν 3345, 1589 cm^{-1}. MS *m/z (%)*: 419 ($M^{\cdot+}$-421,100), 69 (86). HRMS: calcd. for $C_{23}H_{17}BClF_2N_3$ 419.1167; found 419.1175.

1b:

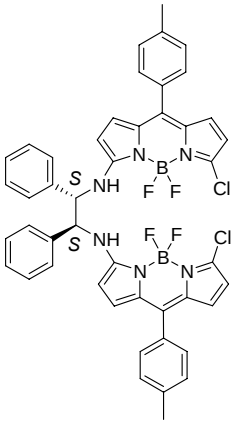

Yield: 42 mg, 50%. $[\alpha]_D^{20}$ +5743.9 (*c* 7.0 x 10^{-2}, $CHCl_3$). For characterization data see enantiomer **1a**.

1c:

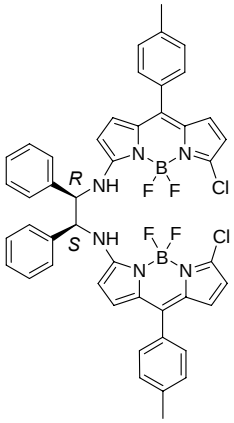

Yield: 45 mg, 53%. R_f = 0.22 (hexane/Et_2O 6:4). ^{1}H NMR ($CDCl_3$, 700 MHz) δ 7.44-7.41 (m, 4H), 7.39-7.34 (m, 6H), 7.31-7.27 (m, 4H), 7.26-7.22 (m, 4H), 6.79 (br s, 2H), 6.75 (d, *J* = 5.0 Hz, 2H), 6.41 (d, *J* = 3.6 Hz, 2H), 6.21 (d, *J* = 3.7 Hz, 2H), 5.84 (d, *J* = 4.9 Hz, 2H), 4.96 (d, *J* = 6.4 Hz, 2H), 2.43 (s, 6H) ppm. ^{13}C NMR ($CDCl_3$, 176 MHz) δ 160.4, 139.6, 136.2, 135.6, 134.0, 132.7, 132.0, 131.1, 130.9, 130.2, 129.5, 129.3, 128.9, 127.1, 121.6, 113.1, 110.3, 63.5, 21.3 ppm. FTIR ν 3383, 1595 cm^{-1}. MS *m/z (%)*: 419 (M^{+}-421, 81), 107 (100). HRMS: calcd. for $C_{23}H_{17}BClF_2N_3$ 419.1167; found 419.1172.

2a:

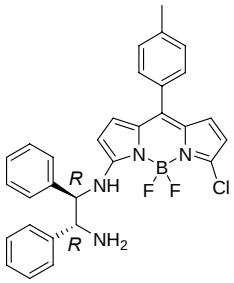

Yield: 40 mg, 38%. R_f = 0.28 (CH_2Cl_2). $[\alpha]_D^{20}$ +270.8 (*c* 0.11, $CHCl_3$). ^{1}H NMR ($CDCl_3$, 300 MHz) δ 8.24 (d, *J* = 7.2 Hz, 1H), 7.55-7.49 (m, 2H), 7.42-7.37 (m, 5H), 7.36-7.29 (m, 3H), 7.27 (d, *J* = 8.1 Hz, 2H), 7.20 (d, *J* = 8.1 Hz, 2H), 6.67 (d, *J* = 5.0 Hz, 1H), 6.34 (d, *J* = 3.9 Hz, 1H), 6.19 (d, *J* = 3.9 Hz, 1H), 5.73 (d, *J* = 5.0 Hz, 1H), 4.71-4.64 (m, 1H), 4.50-4.45 (m, 1H), 2.40 (s, 3H) ppm. ^{13}C NMR ($CDCl_3$, 75 MHz) δ 161.2, 140.1, 139.1, 135.5, 133.2, 132.0, 131.6, 130.9, 130.2, 129.5, 129.1, 128.8, 128.7, 128.1, 128.0, 126.8, 126.3, 119.9, 112.5, 111.6, 63.7, 60.5, 21.3 ppm. FTIR (ATR) ν 3362, 1605 cm^{-1}. MS *m/z (%)*: 526 (M^{+}, 13), 400 (100). HRMS: calcd. for $C_{30}H_{26}BClF_2N_2$ 526.1902; found 526.1903.

2b:

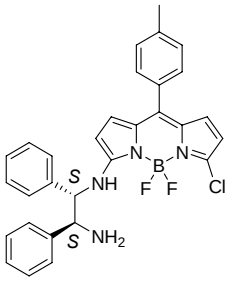

Yield: 40 mg, 38%. $[\alpha]_D^{20}$ –271.6 (*c* 0.10, $CHCl_3$). For characterization data see enantiomer **2a**.

(±)-2c:

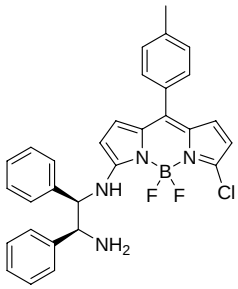

(±)

Yield: 46 mg, 44%. R_f = 0.27 (hexane/Et_2O 1:9). ^{1}H NMR ($CDCl_3$, 300 MHz) δ 7.61 (br s, 1H), 7.35-7.17 (m, 13H include $CDCl_3$), 7.15-7.02 (m, 4H), 6.69 (d, *J* = 5.0 Hz, 1H), 6.35 (d, *J* = 3.9 Hz, 1H), 6.19 (d, *J* = 3.9 Hz, 1H), 5.85 (d, *J* = 5.0 Hz, 1H), 4.80 (m, 1H), 4.49 (d, *J* = 5.3 Hz, 1H), 2.41 (s, 3H) ppm. ^{1}H NMR (CD_3COCD_3, 300 MHz) δ 7.53-7.21 (m, 14H), 6.88 (d, *J* = 5.0 Hz, 1H), 6.49 (d, *J* = 5.1 Hz, 1H), 6.32 (d, *J* = 3.8 Hz, 1H), 6.22 (d, *J* = 3.7 Hz,1H), 5.30-5.24 (m, 2H), 2.43 (s, 3H) ppm. ^{13}C NMR ($CDCl_3$, 75 MHz) δ 161.0, 140.9, 139.2, 137.3, 135.8, 135.4, 133.1, 132.1, 130.9, 130.2, 129.8, 128.9, 128.5, 128.5, 128.2, 128.0, 127.5, 126.9, 120.2, 112.6, 111.5, 63.9, 59.7, 21.3 ppm. FTIR ν 3376, 1598 cm^{-1}. HRMS: calcd. for $C_{30}H_{26}BClF_2N_2$ 526.1902; found 526.1905.

2. Figures and Tables

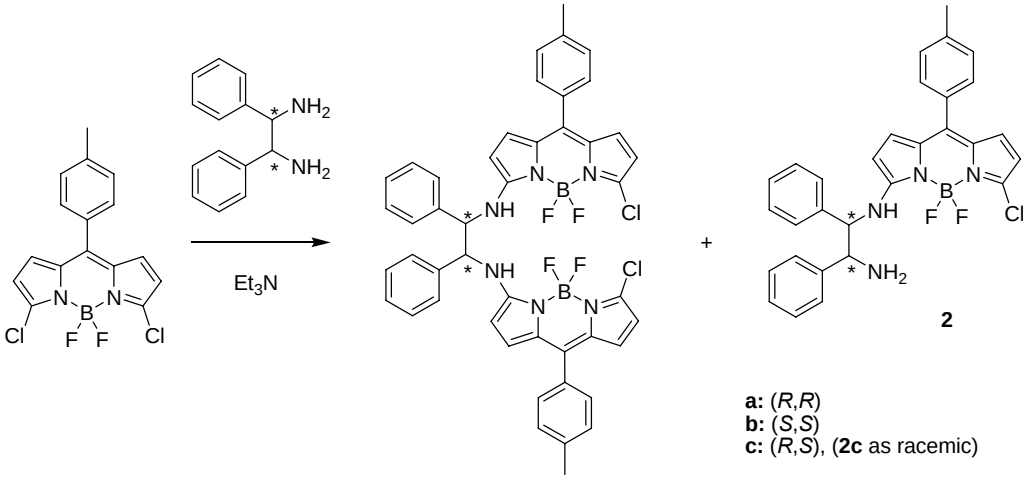

Fig. S1 Synthesis of stereoisomeric bis(BODIPYs) **1** and mono(BODIPYs) **2**.

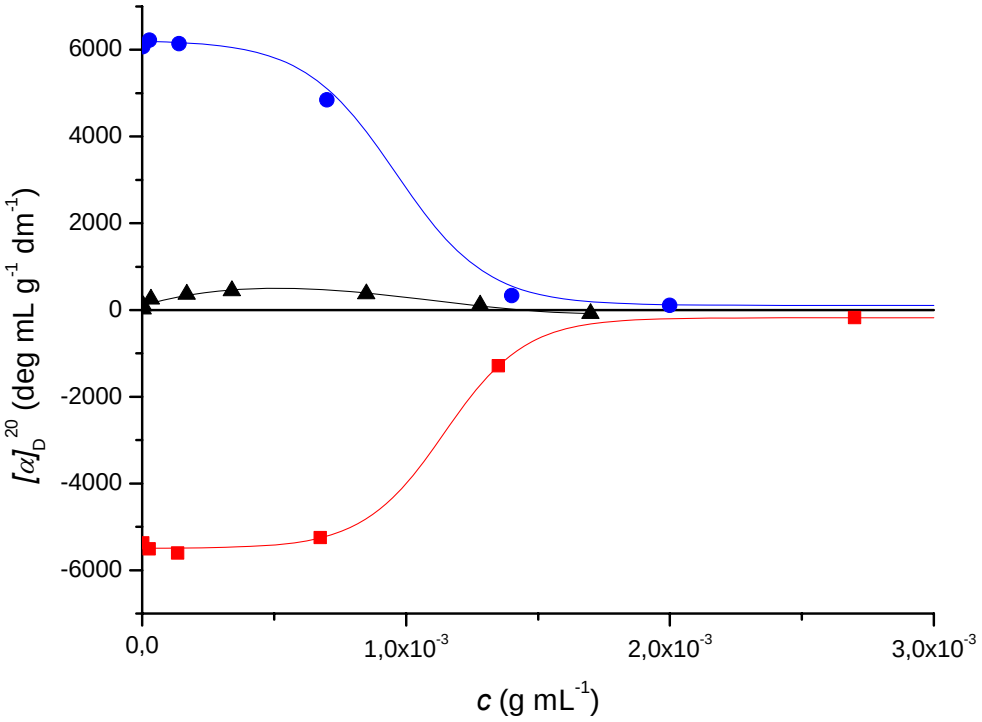

Fig. S2 Optical rotation of **1a** (red), **1b** (blue) and **2a** (black) in $CHCl_3$. Dependence with the concentration (*c*).

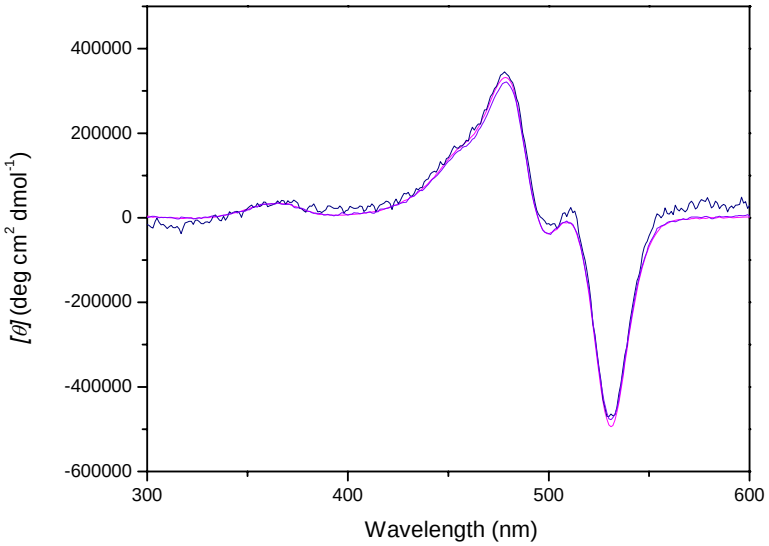

Fig. S3 VC ECD experiment for **1a** in $CHCl_3$ (1.6×10^{-6} M in red, 6.4×10^{-6} M in blue, 1.6×10^{-5} M in black).

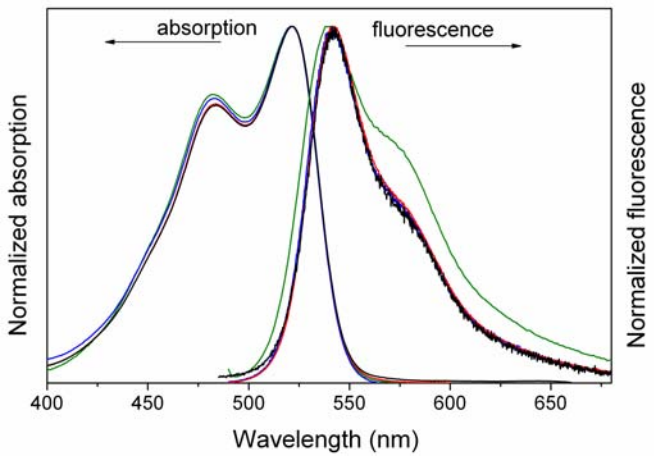

Fig. S4 Variable concentration (VC) photoluminescence experiments for **1b** in CH_2Cl_2 (10^{-6} M in black, 10^{-5} M in red, 10^{-4} M in blue and 10^{-3} M in green). The optical path length was adjusted in each case to avoid inner filter effects as the concentration increases (1 cm, 0.1 cm, 0.01 cm and 0.001 cm, respectively). Recording the fluorescence spectrum with the narrowest cuvette (0.001 cm) was quite difficult due to solvent evaporation and variations in the optical path length during the measurement, explaining the broadening of the emission band at these conditions.

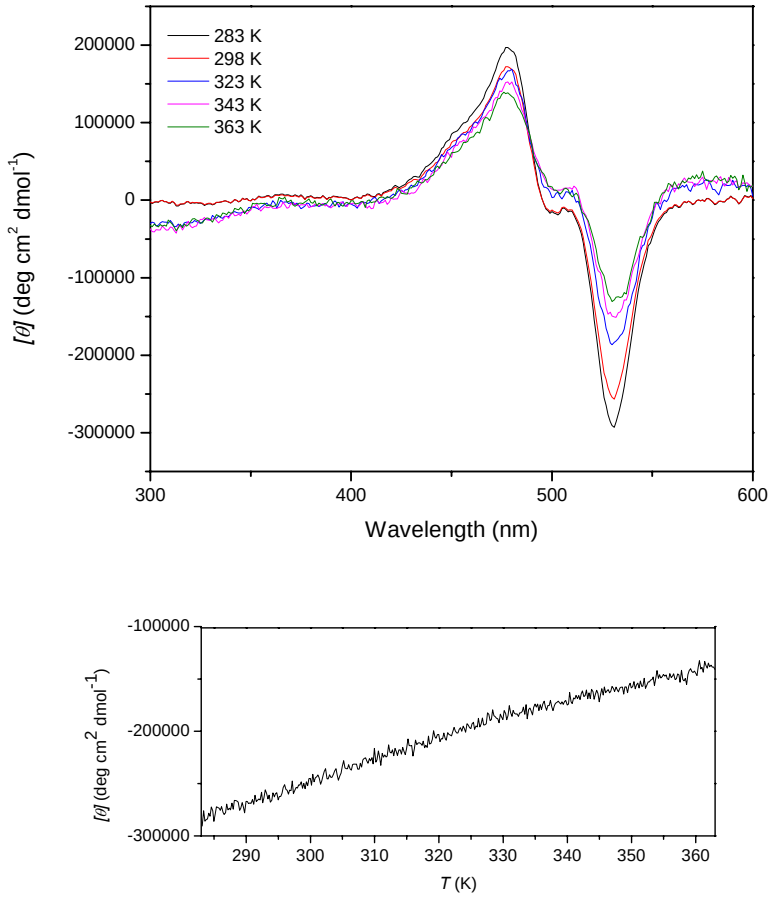

Fig. S5 VT ECD experiments for **1a** in 1,1,2,2-tetrachloroethane (3.7 x 10^{-6} M, above), and corresponding thermal scan at 530 nm (below).

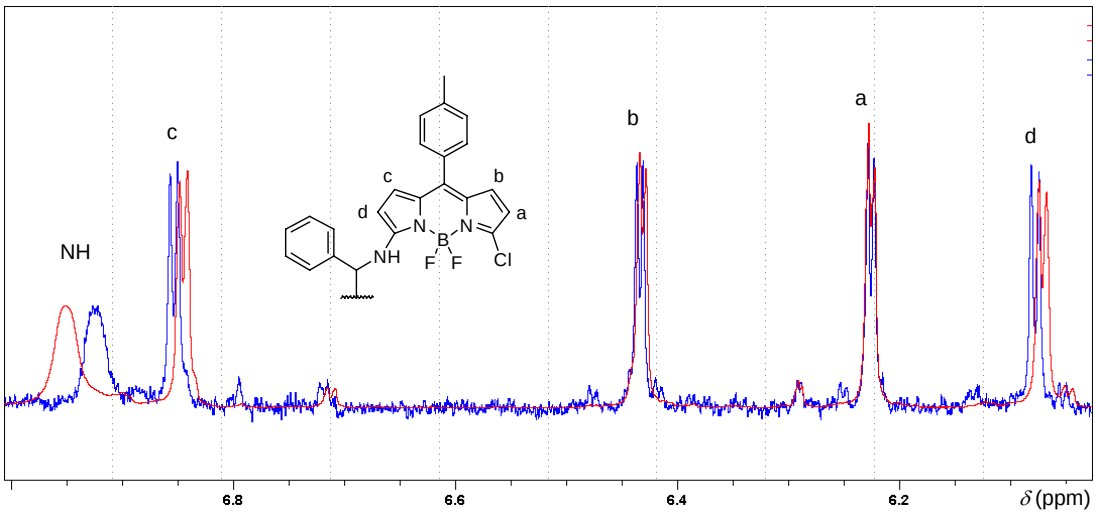

Fig. S6 VC ^{1}H NMR experiment for **1a** in $CDCl_3$ (mobile signals; 4.0 x 10^{-4} M in blue and 1.1 x 10^{-2} M in red).

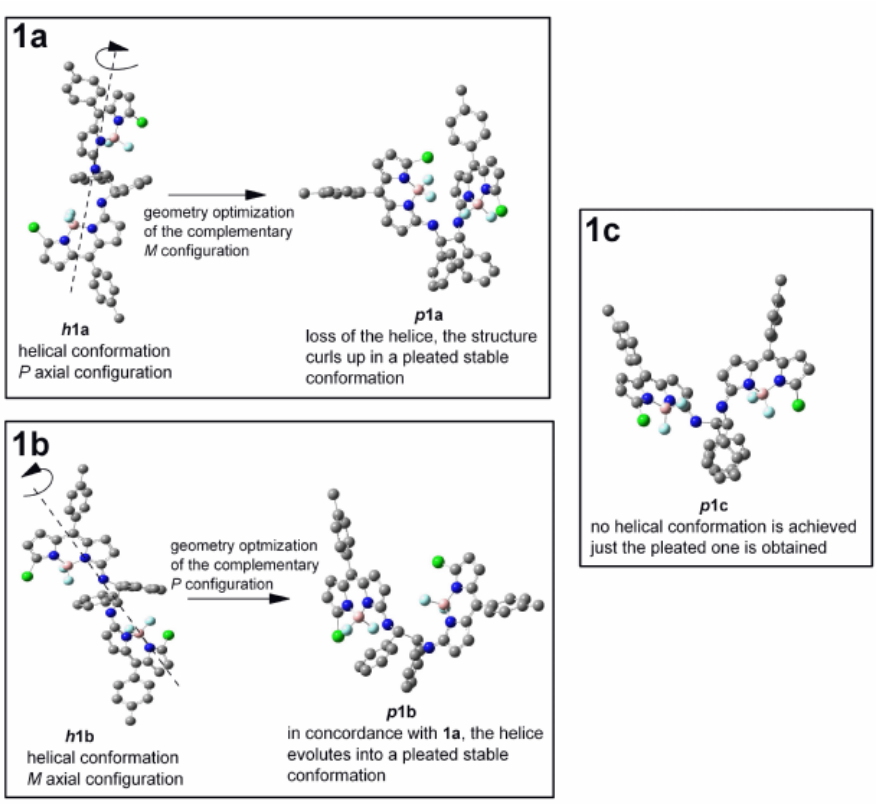

Fig. S7 Computational study on the preferred conformations of **1a**, **1b** and **1c**.

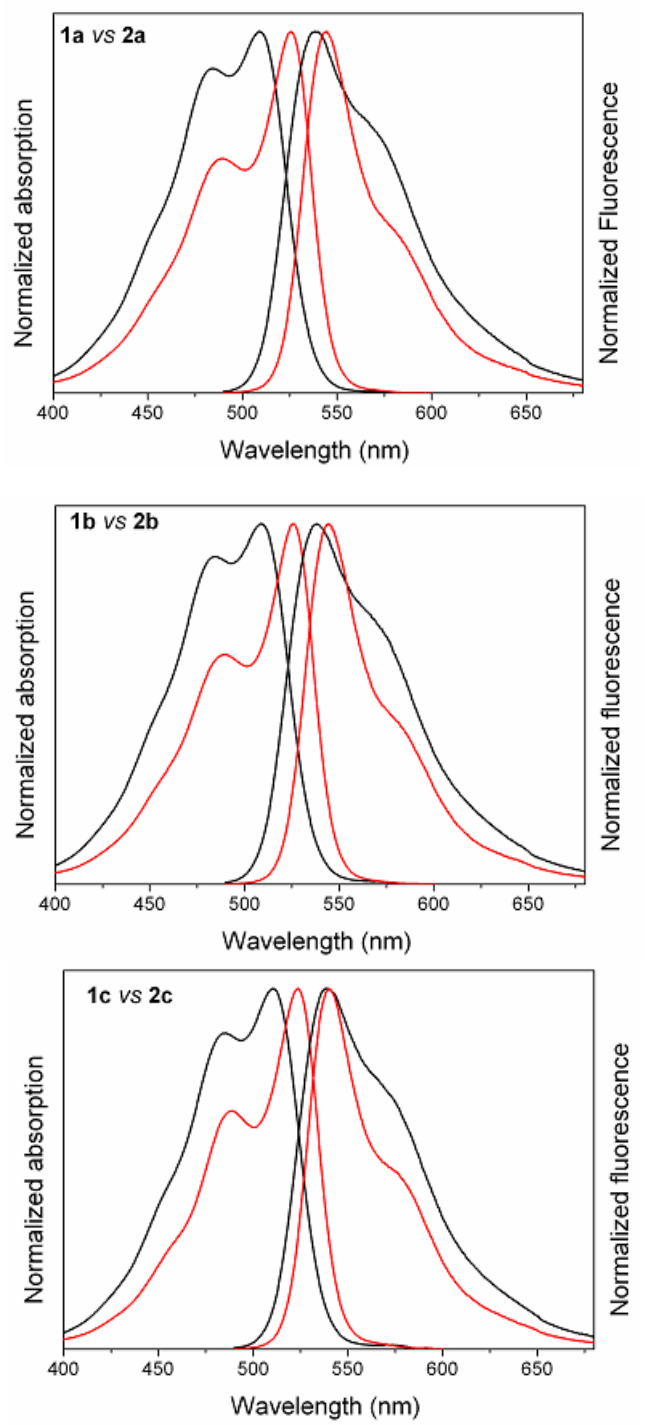

Fig. S8 Comparison of absorption and fluorescence spectra of bis(BODIPYs) **1** (in red) and mono(BODIPYs) **2** (in black) in $CHCl_3$.

Table S1. Ground photophysical data of bis(BODIPYs) **1** and corresponding mono(BODIPYs) **2** in $CHCl_3$. Absorption maximum wavelengths (λ_{ab}) and corresponding molar absorption coefficients (ε_{max}), as well as fluorescence maximum wavelengths (λ_{fl}) and corresponding Stokes shifts ($\Delta\nu_{St}$), fluorescence quantum yields (ϕ) and fluorescence lifetimes (τ).

	λ_{ab} (nm)	ε_{max} (10^4 M^{-1} cm^{-1})	λ_{fl} (nm)	$\Delta\nu_{St}$ (cm^{-1})	ϕ	τ (ns)
1a	525.5	8.3	544.5	665	0.14	0.23 (32%) 1.15 (68%)
1b	525.5	9.4	544.5	665	0.14	0.24 (30%) 1.16 (70%)
1c	523.5	8.9	540.0	585	0.14	0.24 (33%) 1.05 (67%)
2a	508.5	3.9	538.5	1095	0.23	1.20
2b	508.5	3.4	538.0	1080	0.22	1.19
2c	510.5	4.1	538.0	1000	0.20	1.07

3. ^{1}H NMR and ^{13}C NMR Spectra

^{1}H NMR ($CDCl_3$, 300 MHz) spectrum of **1a**

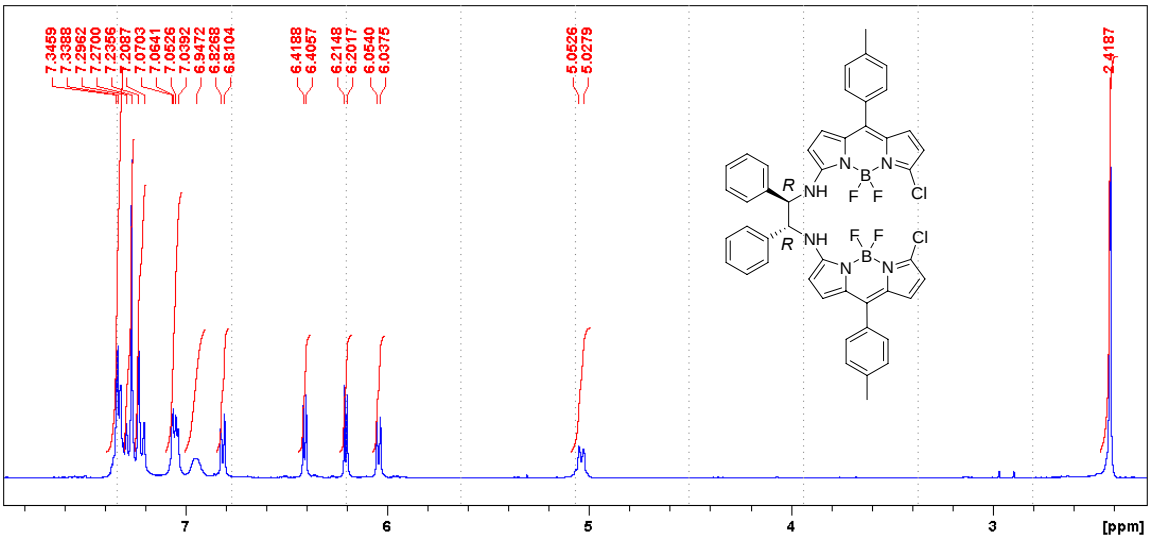

^{13}C NMR ($CDCl_3$, 75 MHz) spectrum of **1a**

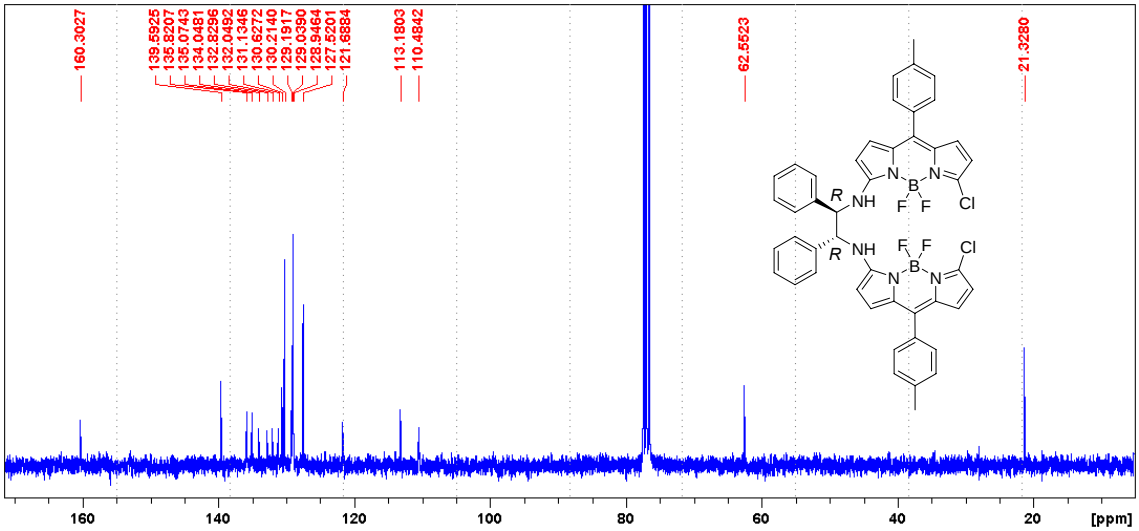

^{1}H NMR ($CDCl_3$, 700 MHz) spectrum of **1c**

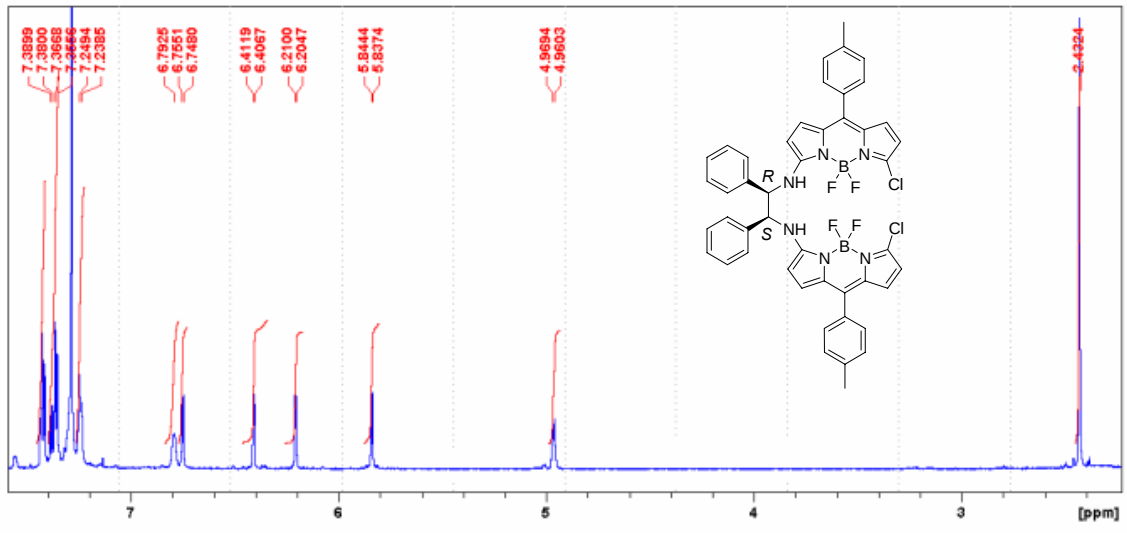

^{13}C NMR ($CDCl_3$, 176 MHz) spectrum of **1c**

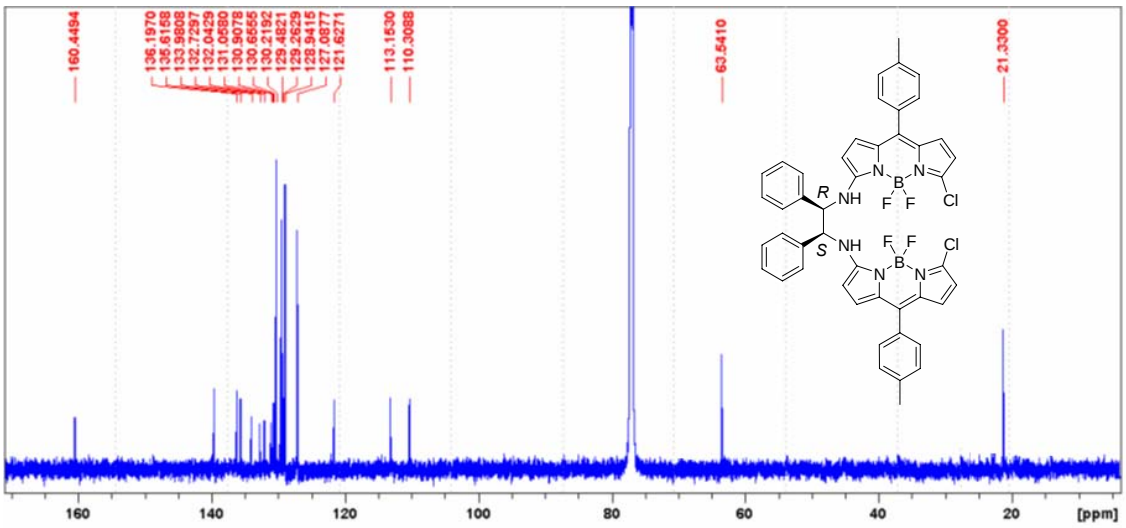

^{1}H NMR ($CDCl_3$, 300 MHz) spectrum of **2a**

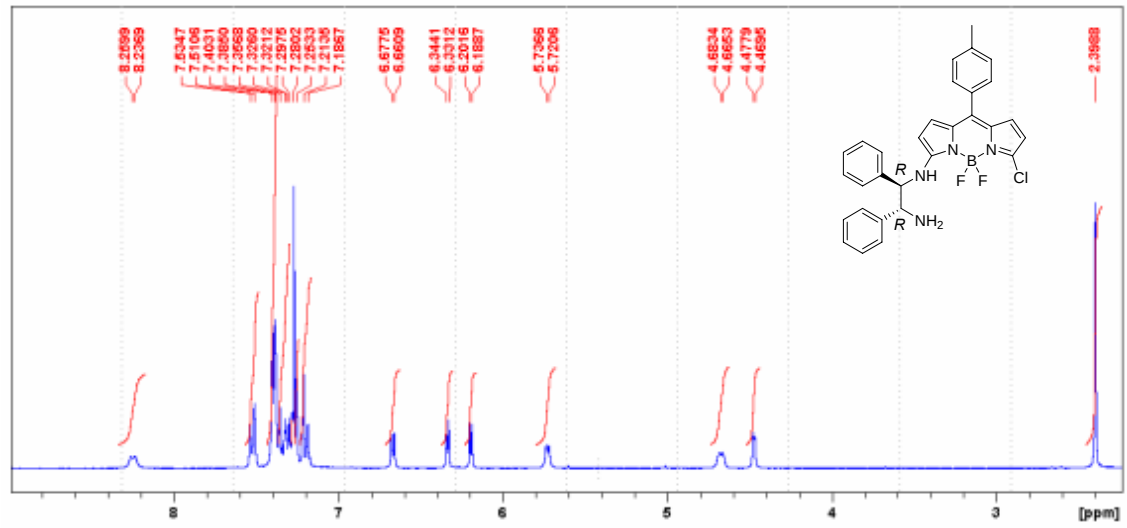

^{13}C NMR ($CDCl_3$, 75 MHz) spectrum of **2a**

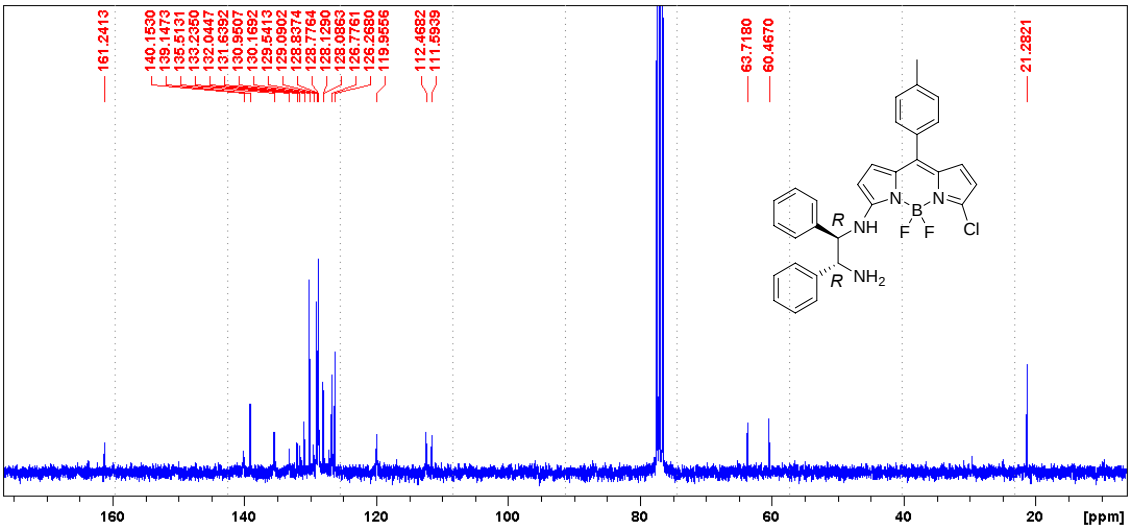

^{1}H NMR ($CDCl_3$, 300 MHz) spectrum of **(±)-2c**

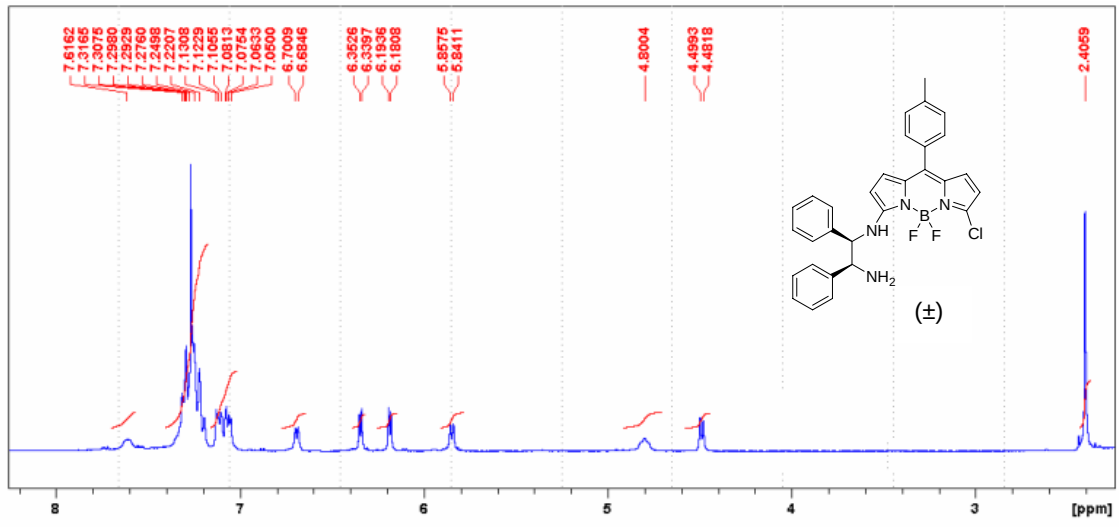

^{13}C NMR ($CDCl_3$, 75 MHz) spectrum of **(±)-2c**